Bull. Inst. Chem. Res., Kyoto Univ., Bol. 62, No. 4, 1984

Dielectric Study of Some Ion-Exchange Resins

Akira ISHIKAWA*, Tetsuya HANAI** and Naokazu KOIZUMI**

Received August 25, 1984

Dielectric measurements were carried out for dense sediments of some ion-exchange beads dispersed in aqueous phases. Dielectric relaxations were observed with relaxation frequencies of the order of 10 kHz to 10 MHz and dielectric increments of the order of 10 to 100 dielectric units. An attempt was made to analyze the observed relaxations by a method which is based on two theories of interfacial polarization. By means of the analysis, reasonable values were determined of the relative permittivities and the electrical conductivities of dispersed ion-exchange beads from the relaxation data of the whole disperse systems. At the same time it was confirmed that the dielectric behavior of the dense sediments of ion-exchange beads was interpreted quantitatively by the theory of interfacial polarization for concentrated suspensions rather than by the theory for dilute suspensions. The deduced permittivities of the ion-exchange beads were lower than those of the outer aqueous phases and were almost unchanged irrespective of differences of dissociation groups, salt forms and salt concentrations in the outer aqueous phases. On the other hand, the deduced conductivities of the beads showed values sensitive to those differences. By using the deduced conductivities of the beads, the binding degrees of counter ions to the fixed charges were estimated for the ion-exchangers adopted. The binding degrees were small for strong acid type ion-exchangers and were specific for weak acid type with high charge density.

KEY WORDS: Counter ions/ Dielectric relaxation/ Electrical conductivity/ Interfacial polarization/ Ion binding/ Ion-exchange resin/ Permittivity/

I. INTRODUTION

One of the important problems in research of ion-exchangers is to elucidate the interaction between fixed charges and ions. It is, however, difficult in general to observe this interaction directly.

The electrical conductivity is a measure relevant to an electrostatic interaction of counter ions with the fixed charges. In many cases, ion-exchangers are available in granular forms or beads with diameter less than 1 mm. Although conductivity measurements can readily be made of ion-exchange beds composed of the closely packed beads and the outer aqueous solutions, accurate calculations of the conductivity of the swollen ion-exchanger from the observed conductivity of the beds are problems which are not satisfactorily solved yet.

Recently a dielectric method was developed[1,2] to determine the permittivity and the conductivity of dispersed particles by means of the analysis of dielectric relaxations caused by interfacial polarization. The results of application of this analysis suggested that the

* 石川 彰: Kao Corporation Tochigi Research Laboratories, 2606, Akabane, Ichikaimachi, Haga, Tochigi 321-34, Japan.

** 花井哲也, 小泉直一: Laboratory of Dielectrics, Institute for Chemical Research, Kyoto University, Uji, Kyoto 611, Japan.

equation for concentrated systems reasonably explained dielectric behavior of several disperse systems such as O/W type emulsions[1,2] and W/O type emulsions.[1,3] It has not yet been well examined whether the method is applicable to general systems consisting of dispersed particles and continuous phases both with the conductivities of appreciable magnitude other than the conventional emulsions of the O/W and W/O types. Thus, dense suspensions of ion-exchange beads are the systems suitable for testing the applicability of the method proposed and for comparing the two theoretical equations.

It has already been reported that suspensions of ion-exchange beads in aqueous solutions show two kinds of dielectric relaxations. One is a low-frequency relaxation as reported by Einolf Jr. and Carstensen[4] with suspensions of acrylic ion-exchange beads. This type of dielectric relaxation is attributed to surface conductivity arising from tangential migration of the ions around the surface of ion-exchange beads, the theories concerned being proposed by O'Konski,[5] Schwarz[6] and Schurr.[7] In this instance, the conductivity of the ion-exchange beads cannot be evaluated from the dielectric relaxation data.

The other is a high-frequency relaxation which may be interpreted as a mechanism of the Maxwell-Wagner relaxation[8] or interfacial polarization. Frolov et al. observed this type of high-frequency relaxations for dilute suspensions of a copolymer of methacrylic acid with ethylene dimethacrylamide.[9] In their study, the observed relaxations were, however, assigned to the relaxation of an ionic region of restricted zones inside the ion-exchange beads rather than the Maxwell-Wagner mechanism.

Spiegler *et al.*[10,11] observed high-frequency relaxations for the beds of Amberlite beads. They obtained the relative permittivity and the electrical conductivity of the resins by means of an analysis based upon their model.[12,13] In view of their simplified model, the values obtained with their method should be subjected to further consideration. Furthermore, systematic data with widely varied conductivity of the outer aqueous phases are necessary on the application of their analysis.

In view of the above situation, the present study is scheduled to obtain detailed information on dielectric behavior of ion-exchange beads in equilibrium with aqueous solutions. The former part of this study is devoted to give a quantitative interpretation to the dielectric relaxations observed for ion-exchange beds. Stress is laid on examination of validity of our analysis and on comparison between the two theoretical equations used for the analysis. The phase parameters concerning ion-exchange beads are successfully evaluated as a result of the data analysis. In the latter part, further considerations are made on dielectric properties of some ion-exchange beads. The interaction between fixed charges and different kinds of counter ions is discussed in terms of the deduced values of the phase parameters.

2. SYMBOLS

The symbols used in this paper are summarized as follows.

- ε relative permittivity
- κ electrical conductivity
- f measuring frequency
- ϵ_v permittivity of free space
- j imaginary unit

ε^* complex relative permittivity given by $\varepsilon^*=\varepsilon-j\kappa/(2\pi f\epsilon_v)$

$\Delta\varepsilon''$ loss factor given by $\Delta\varepsilon''=(\kappa-\kappa_l)/(2\pi f\epsilon_v)$

$\Delta\kappa''$ imaginary part of complex conductivity given by $\Delta\kappa''=2\pi f\epsilon_v(\varepsilon-\varepsilon_h)$

f_0 relaxation frequency corresponding to a half-value point in the dielectric relaxation curve

Φ volume fraction of disperse phase

C_{bed} charge density per unit volume of the bed

X fixed charge density in the ion-exchange beads

p volume fraction of the gel matrix to the bed

v volume fraction of the gel matrix to the beads

λ equivalent ionic conductance

Subscripts

a continuous phase

i disperse phase

h limiting values at high frequencies

l limiting values at low frequencies

bead the ion-exchange beads

int the interstices of the gel matrix

In the present study, the parameters such as ε_a, κ_a, ε_i, κ_i and Φ which represent dielectric properties of constituent phases are collectively called phase parameters. The parameters such as ε_l, ε_h, κ_l, κ_h and f_0 which characterize the whole dielectric relaxation profile are collectively called dielectric parameters.

3. THEORY AND PROCEDURE OF DATA ANALYSIS

3.1 Dielectric theory of disperse systems

For a dilute disperse system of spherical particles with the complex permittivity ε_i^* in the continuous medium with the complex permittivity ε_a^*, Wagner[14] proposed the following equation for the complex permittivity ε^* of the whole system.

$$\varepsilon^*=\varepsilon_a^*\frac{2(1-\Phi)\varepsilon_a^*+(1+2\Phi)\varepsilon_i^*}{(2+\Phi)\varepsilon_a^*+(1-\Phi)\varepsilon_i^*}, \tag{1}$$

where Φ is the volume fraction of the dispersed particles.

Closer consideration revealed that Eq. (1) was in poor agreement with experiments at higher concentrations of the dispersed particles.[15] On the basis of Wagner's equation, Hanai[16,17] derived the following equation which is expected to be applicable to higher concentrations.

$$\frac{\varepsilon^*-\varepsilon_i^*}{\varepsilon_a^*-\varepsilon_i^*}\left(\frac{\varepsilon_a^*}{\varepsilon^*}\right)^{1/3}=1-\Phi. \tag{2}$$

3.2 Procedure of data analysis

3.2.1 Case A: when the whole dielectric relaxation can be measured

The dielectric method of analysis developed in our laboratory[1,2] is summarized as

follows, the equations used in the analysis being shown in Appendix.

First of all, the values of ε_l, ε_h, κ_l and κ_h must be determined from the dielectric relaxation data of the suspensions of ion-exchange beads. Next, the values of κ_a, Φ, ε_i and κ_i are calculated in sequence with the Eqs. (A.1)–(A.4) in the Appendix for the equation for dilute systems, and with Eqs. (A.6) and (A.12)–(A.14) for the equation for concentrated systems using the values of ε_l, ε_h, κ_l, κ_h and ε_a obtained above.

3.2.2 Case B: when the dielectric relaxation shifts to higher frequencies beyond the present range

As pointed out in a detailed study,[15] the relaxation frequency for the interfacial polarization increases with κ_a. In practice, the whole relaxation profile shifted to a megahertz region for specimens with addition of KCl. In this instance, only the values of ε_l, κ_l, ε_a and κ_a can be obtained in the frequency range of the present study. For this case, the data analysis on the basis of Eq. (2) is performed as follows.

Separation of the real and imaginary parts of Eq. (2) gives expressions for the limiting values of the permittivities ε_h and ε_l and the electrical conductivities κ_h and κ_l as[15]

$$\frac{\varepsilon_h-\varepsilon_i}{\varepsilon_a-\varepsilon_i}\left(\frac{\varepsilon_a}{\varepsilon_h}\right)^{1/3}=1-\Phi, \tag{3}$$

$$\varepsilon_l\left(\frac{3}{\kappa_l-\kappa_i}-\frac{1}{\kappa_l}\right)=3\left(\frac{\varepsilon_a-\varepsilon_i}{\kappa_a-\kappa_i}+\frac{\varepsilon_i}{\kappa_l-\kappa_i}\right)-\frac{\varepsilon_a}{\kappa_a}, \tag{4}$$

$$\kappa_h\left(\frac{3}{\varepsilon_h-\varepsilon_i}-\frac{1}{\varepsilon_h}\right)=3\left(\frac{\kappa_a-\kappa_i}{\varepsilon_a-\varepsilon_i}+\frac{\kappa_i}{\varepsilon_h-\varepsilon_i}\right)-\frac{\kappa_a}{\varepsilon_a}, \tag{5}$$

and

$$\frac{\kappa_l-\kappa_i}{\kappa_a-\kappa_i}\left(\frac{\kappa_a}{\kappa_l}\right)^{1/3}=1-\Phi. \tag{6}$$

The value of κ_i can be calculated from Eq. (6) provided that the value of Φ is given. The value of ε_i is calculated from Eq. (4) by using the value of κ_i obtained. In these calculations, it is assumed that the volume fraction Φ is equal to that for a specimen without the addition of salt to the suspending medium.

4. EXPERIMENTAL

4.1 Materials

The ion-exchange beads used were of dextran gel type commercially available from Pharmacia Fine Chemicals and phenol resins available Unitika Co. Ltd. The chemical and physical properties of the ion-exchanger are listed in Table I.

4.2 Preparations

4.2.1 Preconditioning with respect to salt form

Prior to use, the ion-exchange beads supplied were sieved to obtain fractions with a uniform size. The fractions for the respective specimens are summarized also in Table I. The ion-exchange beads sieved were allowed to equilibrate with water at least 5 h and subjected to washing with HCl and NaOH solutions five times, followed by washing with

Table I. Ion-exchange beads used in this study.

Ion-exchanger	Dissociation Group	Fraction (*1) by sieving μm	C_{bed} (*2) equiv dm^{-3}	Diameter (*3) μm
Dextran Gel Ion-Exchanger				
Sephadex G-25	carboxyl groups	105–149	0.001	300
SP-Sephadex C-25	sulfopropyl groups	63– 88	0.234–0.238	90
		42– 53	0.247–0.252	
		88–105		
SE-Sephadex (*4)	sulfoethyl groups	200–240	0.019–0.174	200–300
CM-Sephadex C-25	carboxymethyl groups	74– 88	0.45	
QAE-Sephadex A-25	diethyl (2-hydroxy-propyl) alkylammonium groups	74–105	0.333	
Phenol Resin Ion-Exchanger				
Uniselec UR-30	*N*,*N*-bis (carboxymethyl)-aminomethyl groups	105–149(*5)	0.7(*6)	100–150

*1 Obtained by sieving.
*2 Charge density for ion-exchange beds.
*3 Diameter in a state swollen with water over microscope observation.
*4 Prepared as described in Section 4.2.4.
*5 Sieving was carried out for resin beads in a state swollen with water.
*6 Technical data provided by Unitika Co. Ltd.

distilled water. The washing was completed after the conductivities of the supernatants were reduced to the values of distilled water. Then, the slurries of the ion-exchange beads were immersed in electrolyte solutions and subsequently washed with water; this treatment with electrolytes is called preconditioning hereinafter. Table II lists the diameters of

Table II. Diameter and volume fracfion of dextran gel ion-exchange beads SP-Sephadex and CM-Sephadex
p: volume fraction of dextran gel matrix to beds
v: volume fraction of dextran gel matrix to beads, $v=p/\Phi$.

Salt form	Diameter μm	p	$v=p/\Phi$
	SP-Sephadex C-25		
Na^+	140±20	0.168	0.299
Ca^{2+}	115±15	0.203	0.371
Zn^{2+}	120±15	0.208	0.371
Cu^{2+}	120±15	0.208	0.399
	CM-Sephadex C-25		
Na^+	140±20	0.141	0.258
Ca^{2+}	105±15	0.239	0.478
Zn^{2+}	110±15	0.317	0.580
Cu^{2+}	90±15	0.440	0.944

the SP-Sephadex and CM-Sephadex subjected to different preconditionings with salt solutions.

4.2.2 More dilute suspensions[18,19]

More dilute suspensions were prepared by dispersing the beads in viscous polymer solutions which prevent the beads from sedimentation during the dielectric measurements. The polymers used were Sepharose 4-B for Sephadex G-25 suspensions and Ficoll 400 for SP-Sephadex suspensions. The Sepharose 4-B and Ficoll 400 are commercially available from Pharmacia Fine Chemicals. The Sepharose 4-B solutions were prepared by dissolving with heating the slurries of the Sepharose 4-B into water. These polymer solutions showed no appreciable changes in permittivity and conductivity over the present range of frequency.

4.2.3 Suspensions dispersed in organic solvents[18]

The washed Sephadex G-25 beads were taken to dryness in a vacuum oven at 60°C. The dried beads were then dispersed in the desired organic solvents and washed by decantation thrice with the solvents.

4.2.4 Preparation of SE-Sephadex[20]

Besides the commercial ion-exchange beads, ion-exchange beads with different charge density were prepared by sulfoethylation[21] of Sephadex G-25, which is said to be almost uncharged.[22] The Sephadex G-25 beads available in a dry state were sieved to obtain a fraction between 105–149 μm in diameter. The beads were allowed to swell with water in flasks equipped with stirring blades and reflux condensers at least for 2 h. To these slurries the solid of NaOH were added with stirring and cooling. After 30 min aqueous solutions of sodium 2-bromoethanesulfonate (SBSE) were added dropwise. The reaction mixtures were heated for several hours and then washed with water over glass filters until the conductivities of the filtrates were reduced to those of water. The products (abbreviateated to SE-Sephadex, hereinafter) were dried in vacuo at 60°C. A recipe of the chemical reactions is summarized in Table III.

Table III. Recipe for sulfoethylation of dextran gel beads Sephadex G-25.

Specimen No.	G-25 g	water g	NaOH g	SBES (*1) g	Reaction Time/h	Reaction Temp/°C	C_{bed} (*2) mequiv dm^{-3}	p(*3)	diameter (*4) μm
1	4.86	55	10	6.39	5.5	50	19.3	0.196	200±20
2	4.81	55	24	6.35	5.5	50	60.2	0.163	230±30
3	4.86	55	24	6.38	5.5	70	99.4	0.150	210±20
4	4.87	55	40	6.38	5.5	50	115	0.153	230±30
5	4.86	58	40	12.7	5.5	50	174	0.137	240±20
6(*5)	4.86	55	40	12.7	5.5	70	66.6	0.151	210±20

*1 SBES, sodium 2-bromoethanesulfonate.
*2 C_{bed}, fixed charge density per unit volume of the beds.
*3 p, volume fraction of the gel matrix to the beds.
*4 Average diameter of the beads in equilibrium with water.
*5 During the reaction, the Sephadex G-25 beads were degradated in shape. Most of the broken beads were removed by decantation.

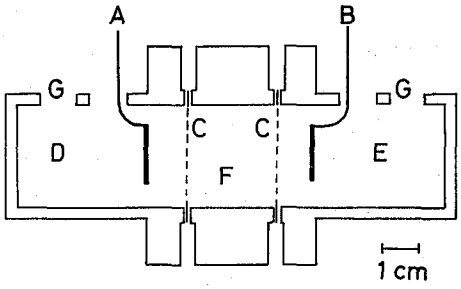

Fig. 1. Apparatus for electrodialysis. A: Anode (Platinum), B: Cathode (Platinum), C: Dialyzing membranes, D: Anode compartment, E: Cathode compartment, F: Specimen compartment, G: Water inlet.

4.2.5 Electrodialysis[18]

To remove ionic impurities, untreated Sephadex G-25 beads were subjected to electrodialysis, the cell for which is shown in Fig. 1. An electric field intensity of 400 V cm^{-1} was applied to the specimen through a pair of electrodes for 4 h. The water in both electrode compartments was renewed with water every 30 min.

4.3 Volume fraction

The volume fraction p of the resin beads to the bed was determined by use of a large tracer molecule which is incapable of entering the beads. The method used was essentially the same as adopted by Einolf *et al.*[23] The tracer molecules used were two polymers, Blue Dextran 2000 and Ficoll 400 available from Pharmacia Fine Chemicals. The mean molecular weights of the Blue Dextran and the Ficoll are 2×10^6 and 4×10^4, respectively.[22] The concentrations of the polymers were determined by optical density measurements at 630 nm for the Blue Dextran and by optical rotatory measurements at 589 nm for the Ficoll.

The volume fraction v of the gel matrix to the whole beads can be calculated from a relation $v=p/\Phi$, where the volume fraction Φ of the suspended beads to the whole disperse system is given from the analysis of dielectric relaxations.

4.4 Charge density

4.4.1 SP-Sephadex, SE-Sephadex and QAE-Sephadex

The fixed charge densities C_{bed} of SP-Sephadex and SE-Sephadex beds were determined by direct titration of the specimens in an acidic form against an NaOH solution.[19,20] The value of C_{bed} of QAE-Sephadex beds was determined by back titration on an OH-form bed with an NaOH solution after addition of an excess amount of an HCl solution.[24] The fixed charge density X of the ion-exchange beads is estimated from the relation $X=C_{bed}/\Phi$. The values of C_{bed} of the SP-Sephadex and QAE-Sephadex are summarized in Table I, and those of SE-Sephadex in Table III.

4.4.2 CM-Sephadex

The fixed charge density C_{bed} of the CM-Sephadex bed in equilibrium with water were estimated from the swelling degree K and the charge density C_w per unit weight of dry beads. The swelling degree defined here is the volume which is occupied by unit weight of dry beads in water. In the case of CM-Sephadex in a sodium form, $K=$ 8.5 cm^3/g and $C_w=4.5$ mequiv/g of the dry beads.[22] Thus, the fixed charge density C_{bed}

per unit volume of beds is estimated from $C_{bed}=C_w/K$ to be 0.529 equiv dm^{-3} in a sodium form. Using the values of Φ determined by the analysis of the dielectric relaxations, the values of X are estimated to be 0.969 equiv dm^{-3} in a sodium form. In the following sections, these values of X in a sodium form will be also used as the values of X in the bivalent ion forms. This approximate estimation for X will draw no erroneous conclusion so far as the discussion of the present study is concerned, in view of the remarkable changes in κ_i which will be shown in Section 5.4.4.

4.5 Dielectric measurements

Dielectric measurements were carried out with a TR-1C transformer Ratio-Arm Bridge of Ando Electric Co. Ltd. and with a 250A RX-meter of Boonton Corporation over a frequency range of 30 Hz to 3 MHz and 1.3 MHz to 130 MHz, respectively. Two types of cells with platinum electrodes of different geometrical shapes were used for the dielectric measurements: one consisted of concentrically cylinderical electrodes and the other consisted of two rod-shaped electrodes. The cell constants and stray capacitances were determined by use of several standard liquids. The residual inductances arising from the terminal leads and the cells were estimated by Schwan's method.[25,26]

5. RESULTS AND DISCUSSION

5.1 Analysis of dielectric relaxation

5.1.1 Low-frequency relaxation

Figure 2 shows the frequency dependence of the permittivity ε, the conductivity κ and the loss factor $\Delta\varepsilon''$ observed for beds of Sephadex G-25 (low fixed charge density type) and SP-Sephadex (high fixed charge density type) dispersed in water. The complex plane plots with the same data are shown in Fig. 3. For disperse systems of particles with fixed charges, two kinds of dielectric relaxations are expected to take place. The relaxations observed in a lower frequency region (called low-frequency relaxation hereafter) are considered to be caused by surface conductivity originating from ions in diffuse double layer. The relaxations in a higher frequency range (high-frequency relaxation) are thought to be due to interfacial polarization mechanism.

The relaxations of the first mechanism have already been observed[27-32] and discussed theoretically by Einolf Jr. and Carstensen,[4] Schwarz[6] and Schurr.[7] According to their studies, the relaxation frequency f_s is given by

$$f_s=\frac{ukT}{\pi R^2 e}, \tag{7}$$

where R, e, u, k and T are the radii of the dispersed particles, the electric charge of the counter ions, the ionic mobility, the Boltzmann's constant and the temperature, respectively. For the present ion-exchange beads, the radii of the beads lie in a range of 10 μm to 100 μm. Thus, the relaxation frequency f_s is estimated to be 10 mHz to 1 Hz by using the value of the ionic mobility of sodium ions in aqueous solutions. Therefore, the dielectric relaxations found in Fig. 2 are not attributable to the surface conductivity, but should be assigned to interfacial polarization.

In Fig. 2 are seen very gradual decrease in κ and abrupt increase in ε with decreasing

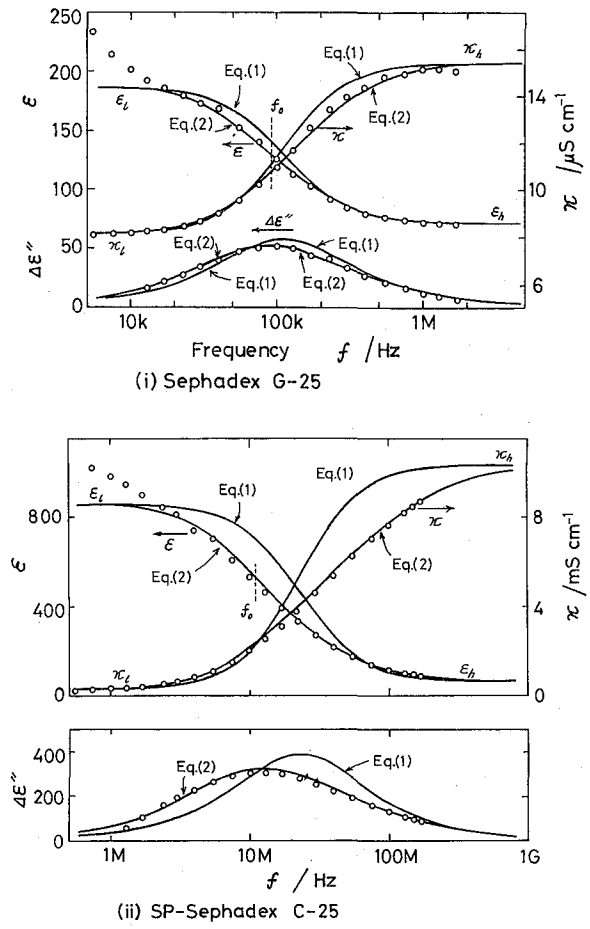

Fig. 2. Frequency dependence of relative permittivity ε, electrical conductivity κ, and loss factor $\Delta\varepsilon''=(\kappa-\kappa_l)/(2\pi f\epsilon_v)$ for beds of (i) Sephadex G-25 beads in a sodium form dispersed in water at 22.4°C and (ii) SP-Sephadex C-25 beads in a sodium form dispersed in water at 24.0°C.

frequency f at lower frequencies. This phenomenon may be attributed to electrode polarization[33,34] and/or to the tailing of another relaxation mechanism in a lower frequency range.

In the present study, only the high-frequency relaxations will be discussed, since the permittivity and the conductivity of the ion-exchange beads are deduced from the high-frequency relaxations rather than from the low-frequency relaxations.

5.1.2 Analysis of high-frequency relaxation

The observed dielectric relaxations in Fig. 2 were analyzed following the procedure of Case A in Section 3.2.1. Table IV summarizes the values of κ_a, Φ, ε_i, κ_i and f_0 calculated on the basis of Eqs. (1) and (2) using the observed values of ε_l, ε_h, κ_l, κ_h and ε_a.

Comparison between Eqs. (1) and (2)

In the case of Sephadex G-25, the values of κ_a calculated from Eqs. (1) and (2) seem

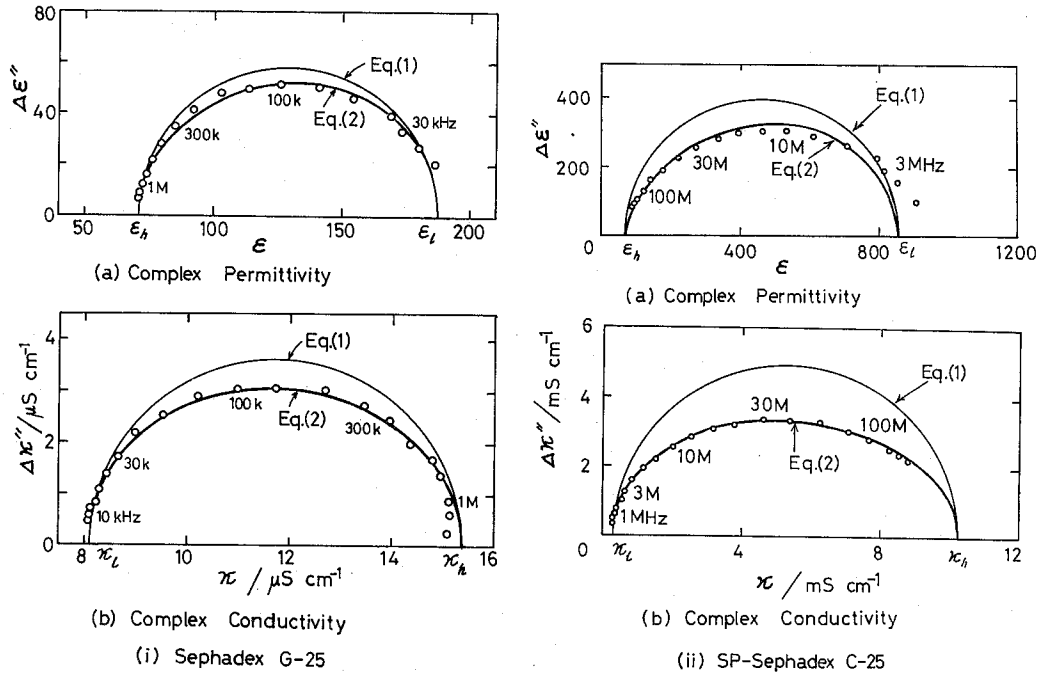

Fig. 3. Complex plane plots of complex relative permittivity and complex conductivity for beds of (i) Sephadex G-25 beads in a sodium form dispersed in water at 22.4°C and (ii) SP-Sephadex C-25 beads in a sodium form dispersed in water at 24.0°C. Theoretical curves are claculated from Eqs. (1) and (2). Numbers beside observed points are measuring frequencies.

to be in fairly good agreement with the conductivity measured directly with the supernatant. However, in the case of SP-Sephadex the values of κ_a deduced from Eqs. (1) and (2) are about ten times larger than the values κ_a of the supernatants. As mentioned above, this may be due to the fact that the observed values of κ_l are greatly raised by another low-frequency relaxation mechanism located at lower frequencies.[19]

The volume fractions were determined by using tracer molecules to be $\Phi_{tracer}=0.62\pm0.01$ both for Sephadex G-25 and SP-Sephadex. Electron microscope observation[22] revealed that the surface of the Sephadex G-25 beads was uneven as schematically depicted in Fig. 4. The tracer molecules seem to be too large to migrate into the creases on the surface of the Sephadex G-25 beads. The volume fractions Φ_{tracer} are, therefore, expected to be larger than those determined from dielectric measurements. These results indicate that the volume fractions Φ deduced from Eq. (2) for Sephadex G-25 and SP-Sephadex are reasonable values. On the other hand, the value of Φ deduced from Eq. (1) for SP-Sephadex is too large in magnitude, indicating unsuitable application of Eq. (1) to the present systems.

The values of ε_i of the Sephadex G-25 and SP-Sephadex beads are smaller than those of ε_a. This finding is consitent with the swollen state of the bead, which is regarded as a mixture of two components: one is the framework or gel matrix and the other is the interstitial water whose permittivity is considered to be larger than that of the gel matrix.

Table IV. Dielectric parameters observed for beds of (i) Sephadex G-25 beads in a sodium form dispersed in water at 22.4°C and (ii) SP-Sephadex beads in a sodium form dispersed in water at 24.0°C and the respective phase parameters calculated from Eqs. (1) and (2).

(i) Sephadex G-25 bed at 22.4 °C.

Observed Values			Values calculated from Eq. (1)	Values calculated from Eq. (2)
ε_a	76.1			
κ_a/μS cm^{-1}	1.90	κ_a/μS cm^{-1}	2.16	1.76
dielectric parameters		Φ	0.630	0.562
ε_l	187.8	ε_i	67.8	66.8
ε_h	70.8	κ_i/μS cm^{-1}	22.6	25.1
κ_l/μS cm^{-1}	8.10			
κ_h/μS cm^{-1}	15.4			
f_0/kHz	94.7	f_0/kHz	112	92.0

(ii) SP-Sephadex C-25 bed at 24.0°C.

Observed Values			Values calculated from Eq. (1)	Values calculated from Eq. (2)
ε_a	76.0			
κ_a/μS cm^{-1}	2.35	κ_a/μS cm^{-1}	26.3	25.6
dielectric parameters		Φ	0.783	0.568
ε_l	855.6	ε_i	63.8	59.4
ε_h	66.3	κ_i/mS cm^{-1}	12.8	16.9
κ_l/mS cm^{-1}	0.303			
κ_h/mS cm^{-1}	10.3			
f_0/MHz	13.1	f_0/kHz	22.8	13.8

The observed value of f_0 is closer to that calculated from Eq. (2) for concentrated systems than to that from Eq. (1) for dilute systems.

Theoretical curves of the frequency dependence of ε, κ and $\Delta\varepsilon''$ and the complex plane plots of $\Delta\varepsilon''$ against ε were calculated[35] from Eqs. (1) and (2) by using the deduced phase parameters, being compared with the observed data in Figs. 2 and 3. The observed data are closer to the theoretical curves given by Eq. (2) than to those by Eq. (1). From these results it is obvious that the high-frequency relaxations in Fig. 2 are explained more

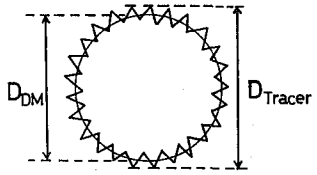

Fig. 4. Effective volume of an ion-exchange bead. D_{DM}: Effective diameter for dielectric measurements. D_{Tracer}: Effective diameter for tracer molecules.

quantitatively by Eq. (2) than by Eq. (1).

Dilute Suspension

To examine the validity of the present analysis, dielectric measurements were carried out for suspensions of Sephadex G-25 and SP-Sephadex in three more dilute concentrations of the dispersed beads. Table V summarizes the observed and deduced dielectric data with these suspensions. The observed values of f_0 in Table V shift to higher frequencies with dilution as expected from Eqs. (1) and (2),[15] and are in better agreement with the values calculated from Eq. (2) than with those from Eq. (1). The values of Φ calculated from Eq. (2) decrease in conformity with the respective dilutions, whereas the values ε_i and κ_i remain unchanged irrespective of dilution and agree well with those shown in Table IV. These consistent results suggest that Eq. (2) is reasonably applied to the dense sediments of the Sephadex G-25 and the SP-Sephadex by our method of analysis.

5.2 Phase Parameters Deduced

5.2.1 Gel beads subjected to preconditionings with salt solutions

Dielectric measurements were carried out for densely packed sediments of low fixed charge density type Sephadex G-25 beads which were subjected to the respective preconditionings with different kinds of salt solutions and subsequently dispersed in water.

Table V. Dielectric parameters observed for (i) Sephadex G-25 suspensions in Sepharose 4-B aqueous solutions with ε_a=79.5 at 23.9°C and (ii) SP-Sephadex C-25 in Ficoll 400 aqueous solutinos with ε_a=65.4 at 24.8°C and phase parameters respectively calculated from Eqs. (1) and (2).

(i) Sephadex G-25 suspensions in aqueous Sepharose solutions.

Specimen \ Dilution	A 1	B 4/5	C 3/5
	Observed values		
ε_l	102.5	96.6	91.8
ε_h	72.6	73.6	74.9
κ_l/μS cm^{-1}	10.9	10.3	9.47
κ_h/μS cm^{-1}	14.3	13.3	11.7
f_0/kHz	188	204	213
	Values calculated by Eq. (1)		
κ_a/μS cm^{-1}	5.67	6.20	6.40
Φ	0.471	0.373	0.302
ε_i	65.3	64.3	64.9
κ_i/μS cm^{-1}	22.9	23.6	22.5
f_0/kHz	203	231	240
	Values calculated by Eq. (2)		
κ_a/μS cm^{-1}	4.87	5.60	5.98
Φ	0.495	0.400	0.328
ε_i	66.0	65.3	66.0
κ_i/μS cm^{-1}	22.8	23.3	22.1
f_0/kHz	188	218	230

(ii) SP-Sephadex C-25 suspensions in Ficoll aqueous solutions

Specimen \ Dilution	A 1	B 3/4	C 1/2
	Observed values		
ε_l	378	200	134
ε_h	60	63	64
κ_l/mS cm^{-1}	0.451	0.256	0.205
κ_h/mS cm^{-1}	8.45	5.42	3.78
f_0/MHz	33	59	79
	Values calculated by Eq. (1)		
κ_a/μS cm^{-1}	75	81	98
Φ	0.64	0.42	0.27
ε_i	57	60	60
κ_i/mS cm^{-1}	13	12	13
f_0/MHz	45	68	92
	Values calculated by Eq. (2)		
κ_a/μS cm^{-1}	73	81	98
Φ	0.47	0.33	0.22
ε_i	54	58	59
κ_i/mS cm^{-1}	17	16	16
f_0/MHz	31	54	79

The Sephadex G-25 is said to carry a small amount of carboxyl groups.[36] All the specimens exihibited the high-frequency relaxations similar to that of the specimen of Fig. 2-(i). The observed data were analyzed with the procedure of Case A in Section 3.2.1 to evaluate the phase parameters. The results are shown in Table VI together with the observed dielectric parameters. The permittivities ε_i and the volume fractions Φ of the gel beads were unchanged irrespective of the preconditionings, while the conductivities κ_i of the beads showed values characteristic of the respective preconditionings. Figure 5 shows the schematic diagram of sequence of the preconditionings and the associated values of κ_i in parentheses. The value of κ_i for the specimen preconditioned with an HCl solution is appareciably large in comparison with that for an untreated specimen. The values of κ_i for the beads preconditioned with NaCl and NaOH solutions after the HCl treatment are both in good agreement with value of κ_i for the untreated specimen. Thus, the magnitude of κ_i is seen to be characterized not by the anion species but by the cation species in solutions used for the preconditionings.

These very characteristic results on κ_i can be interpreted reasonably in terms of ion-exchange resins. The carboxyl groups fixed to the gel matrix are accompanied by the same amount of their counter cations even after thorough washing with water. These counter cations play the main part in the conductivity of the swollen gel beads. Therefore, the untreated specimen is considered to be in a sodium form with respect to its counter ions. Contrary to the expectation from removal of ionic impurities, the specimen subjected to the electrodialysis is inferred to be in a hydrogen ion form, since the specimen showed the same high conductivity κ_i as shown by the specimen treated with an HCl solution.

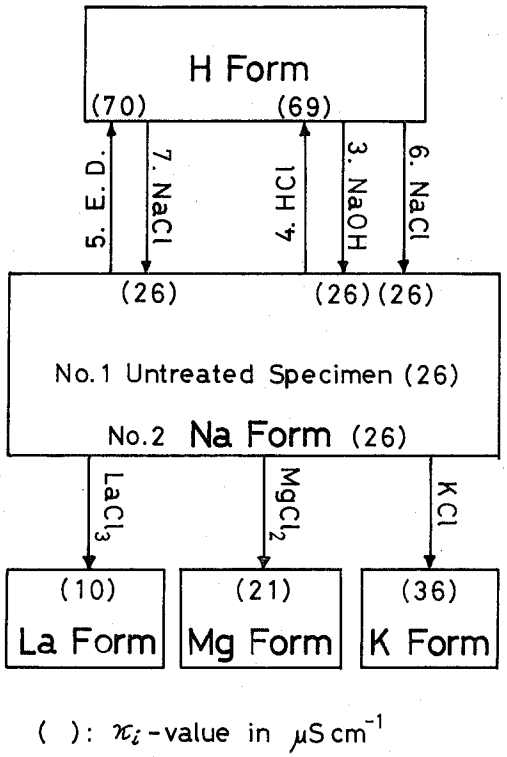

Fig. 5. Schematic diagram of preconditionings and the associated values of κ_i for Sephadex G-25 beads at 24.5°C. Values of κ_i in μS cm^{-1} are shown in parentheses. The preconditionings are shown in Table VI.

In the initial stage of the electrodialysis, ionic impurities are removed, so that the only ions remaining in the gel beads are the fixed charges and their counter cations. Further application of the electric field causes the counter cations to flow out, and the cation sites are subsequently occupied by hydrogen ions generated by dissociation of water molecules around the fixed charges.

To examine the effect of preconditionings on the phase parameters also for anion-exchange resins,[24] dielectric measurements were carried out for beds of quarternary ammonium type dextran gel ion-exchanger QAE-Sephadex A-25 which were subjected to the preconditionings with different electrolyte solutions and subsequently dispersed in water. The QAE-Sephadex beds exhibited the similar high-frequency relaxations as observed for the specimen of Fig. 2-(ii). Table VII summarizes the dielectric parameters observed and the phase parameters evaluated through the analysis. Just like the case of Sephadex G-25, the values of Φ and ε_i of the QAE-Sephadex beads are almost unchanged irrespective of the preconditionings, while the values of κ_i show values characteristic of the preconditionings. Figure 6 is a schematic diagram of the preconditionings and the associated values of κ_i. In contrast to the Sephadex G-25 beds, the magnitude of κ_i of QAE-Sephadex is evidently determined by the anion species of electrolytes used in the final steps of the respective treatments.

Table VI. Dielectric parameters observed for Sephadex G-25 beds subjected to ion conversion treatments at 24.5°C and phase parameters calculated from Eq. (2).

Treatment No.	Observed Dielectric Parameter							Calculated Phase Parameter				
	ε_l	ε_h	$\frac{\kappa_l}{\mu S\ cm^{-1}}$	$\frac{\kappa_h}{\mu S\ cm^{-1}}$	$\frac{f_0}{kHz}$	ε_a	$\frac{\kappa_a}{\mu S\ cm^{-1}}$	$\frac{\kappa_a}{\mu S\ cm^{-1}}$	Φ	ε_i	$\frac{\kappa_i}{\mu S\ cm^{-1}}$	$\frac{f_0}{kHz}$
1. Untreated	248.7	72.4	7.02	15.8	76.1	79.3	1.25	1.25	0.571	67.5	25.5	69.6
2. NaCl	164.0	72.9	9.94	16.5	108	79.0	2.30	2.37	0.581	68.7	25.7	108
3. NaOH	223.6	72.7	7.83	16.2	84.3	80.5	1.98	1.53	0.570	67.1	26.0	79.2
4. HCl	316.2	71.7	15.0	42.1	162	79.0	1.18	2.30	0.566	66.3	69.3	149
5. E.D.	248.5	72.5	19.5	43.5	214	79.9	1.70	3.49	0.572	67.3	70.1	191
6. HCl, NaCl	272.2	73.0	6.87	16.3	68.6	79.9	1.51	1.15	0.574	68.1	26.3	65.4
7. E.D., NaCl	234.2	72.7	7.56	16.0	78.6	79.9	1.49	1.40	0.575	67.7	25.7	74.3

Treatment No. 1. as purchased and untreated. 2. treated with NaCl solution. 3. treated with NaOH solution
4. treated with HCl solution. 5. subjected to electrodialysis. 6. treatment with NaCl solution after preconditioning with HCl solution
7. treatment with NaCl solution after electrodialysis.

Table VII. Dielectric parameters observed for QAE-Sephadex beds subjected to ion conversion treatments with electrolyte solutions at 25.0°C and phase parameters calculated from Eq. (2).

Treatment No.	Observed Dielectric Parameter							Calculated Phase Parameter				
	ε_l	ε_h	$\frac{\kappa_l}{mS\ cm^{-1}}$	$\frac{\kappa_h}{mS\ cm^{-1}}$	$\frac{f_0}{MHz}$	ε_a	$\frac{\kappa_a}{\mu S\ cm^{-1}}$	$\frac{\kappa_a}{\mu S\ cm^{-1}}$	Φ	ε_i	$\frac{\kappa_i}{mS\ cm^{-1}}$	$\frac{f_0}{MHz}$
1. NaCl	691	67	0.296	11.0	20.0	77.6	3.91	31.9	0.531	58.4	19.1	19.5
2. HCl	656	68	0.327	11.1	20.5	77.8	6.20	37.1	0.523	59.8	19.5	20.9
3. NaOH	612	68	1.60	22.6	50.2	78.6	2.68	185	0.531	59.4	39.0	44.9
4. NaCl, NaOH	593	68	1.06	21.3	48.3	77.5	7.30	129	0.516	59.8	38.0	45.1
5. NaOH, NaCl	652	68	0.252	10.8	20.4	78.7	2.58	29.4	0.517	58.9	19.1	20.7
6. NaOH, HCl	645	67	0.252	11.0	21.2	78.9	7.61	29.7	0.515	56.9	19.3	21.2

Treatment No. 1. treated with NaCl solution. 2. treated with HCl solution. 3. treated with NaOH solution.
4. treated with NaOH solution after preconditioning with NaCl. 5. treated with NaCl solution after preconditioning with NaOH.
6. treated with HCl solution after preconditioning with NaOH.

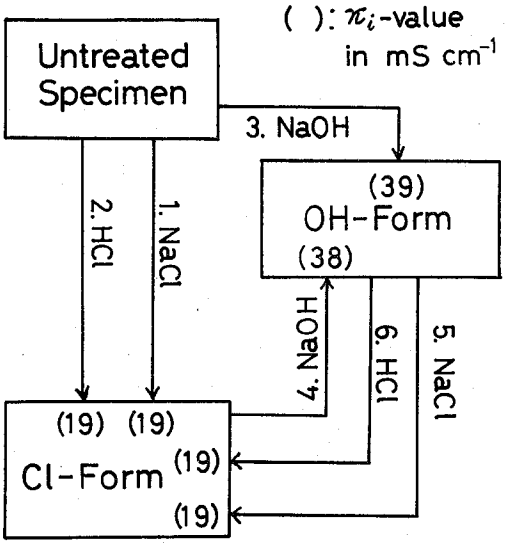

Fig. 6. Schematic diagram of preconditionings and the associated values of κ_i for QAE-Sephadex A-25 resins at 25.0°C. Values of κ_i in mS cm^{-1} are shown in parentheses. The preconditionings are shown in Table VII.

5.2.2 Phase parameters of ion-exchange beds with different salt forms

In order to examine characteristics of dissociation groups, dielectric measurements were carried out for beds of dextran gel ion-exchange beads with the following different types of fixed charges: sulfoxyl groups with high fixed charge density (SP-Sephadex);[19] carboxyl groups with low fixed charge density (Sephadex G-25)[18] and high fixed charge density (CM-Sephadex); quarternary ammonium groups with high fixed charge density (QAE-Sephadex).[24] All the beds of these ion-exchange beads in water showed the similar high-frequency relaxations as shown in Fig. 2. In Tables VIII to X are summarized the dielectric parameters of the observed high-frequency relaxations and the phase parameters deduced by the procedure of Case A.

Validity of the analysis is assured by the satisfactory agreement between the observed and calculated values of f_0 in Tables VIII to X. As seen in Tables IV-(i), V-(i) and VII, the values of Φ remain unchanged irrespective of the salt forms. This fact indicates that the packing degree is independent of the salt forms.

The values of ε_i in Tables VIII to X also remain unchanged irrespective of the salt form, being smaller than ε_a of water. The relative magnitude of ε_i to ε_a is in accord with Spiegler's result for an Amberlite ion-exchange resin.[10,11] On the other hand, the value of κ_i is closely dependent upon the salt form.

5.2.3 Phase parameters of beds of phenol resin ion-exchangers

Dielectric measurements were carried out for a bed of phenol resin ion-exchange beads Uniselec UR-30 in a hydrogen form dispersed in water. Frequency dependence and complex plane plots are shown in Figs. 7 and 8, respectively. The observed dielectric parameters and calculated phase parameters are summarized in Table XI.

Table VIII. Dielectric parameters observed for beds of Sephadex G-25 beads in different salt forms dispersed in water at 24.5°C and phase parameters calculated from Eq. (2).

Salt form	Observed Dielectric Parameter							Calculated Phase Parameter				
	ε_l	ε_h	$\frac{\kappa_l}{\mu S\ cm^{-1}}$	$\frac{\kappa_h}{\mu S\ cm^{-1}}$	$\frac{f_0}{kHz}$	ε_a	$\frac{\kappa_a}{\mu S\ cm^{-1}}$	$\frac{\kappa_a}{\mu S\ cm^{-1}}$	Φ	ε_i	$\frac{\kappa_i}{\mu S\ cm^{-1}}$	$\frac{f_0}{kHz}$
H^+	316.2	71.7	15.0	42.1	162	79.0	1.18	2.30	0.566	66.3	69.3	149
Rb^+	228.9	71.1	12.0	26.7	138	79.2	2.56	2.36	0.555	65.0	43.8	132
K^+	254.3	72.4	9.80	22.4	103	80.8	1.24	1.75	0.569	66.5	36.1	96.7
Na^+	248.7	72.4	7.02	15.8	76.1	79.3	1.25	1.25	0.571	67.5	25.5	69.6
Li^+	163.2	72.6	8.11	13.3	88.9	80.6	1.36	1.95	0.586	67.2	20.4	86.7
NH_4^+	216.8	70.0	11.1	24.6	133	78.7	2.21	2.33	0.540	63.1	40.9	132
Me_4N^+	144.7	70.7	9.65	15.3	117	78.5	2.16	2.61	0.568	65.2	23.7	117
$n\text{-}Bu_4N^+$	123.5	71.3	5.49	7.86	75.2	79.5	1.62	1.75	0.568	65.5	11.9	72.1
$n\text{-}Am_4N^+$	133.0	72.1	5.57	8.22	73.1	80.3	1.39	1.64	0.575	66.4	12.5	70.0
Mg^{2+}	179.1	71.4	7.18	13.2	87.8	78.9	1.73	1.68	0.555	65.7	21.4	83.4
Ca^{2+}	129.1	72.0	8.52	12.3	108	79.4	2.38	2.52	0.585	67.0	18.5	104
Sr^{2+}	163.8	71.0	8.25	14.1	99.6	79.4	2.00	2.03	0.568	65.1	22.1	94.4
Ce^{3+}	102.4	72.5	4.85	6.14	71.5	79.0	2.02	1.91	0.571	67.8	9.00	71.4
La^{3+}	101.4	72.8	5.42	6.83	81.3	79.4	2.07	2.21	0.562	68.0	10.1	81.7

Table IX. Dielectric parameters observed for beds of SP-Sephadex beads in different salt forms dispersed in water at 24.0°C and phase parameters calculated from Eq. (2).

Salt form	Observed Dielectric Parameter							Calculated Phase Parameter				
	ε_l	ε_h	$\frac{\kappa_l}{\text{mS cm}^{-1}}$	$\frac{\kappa_h}{\text{mS cm}^{-1}}$	$\frac{f_0}{\text{MHz}}$	ε_a	$\frac{\kappa_a}{\mu\text{S cm}^{-1}}$	$\frac{\kappa_a}{\mu\text{S cm}^{-1}}$	Φ	ε_i	$\frac{\kappa_i}{\text{mS cm}^{-1}}$	$\frac{f_0}{\text{MHz}}$
H^+	835	63	1.36	56.3	79.9	74.6	1.26	117	0.565	54.8	91.5	77.3
Rb^+	808	62	0.536	16.0	21.9	73.5	2.77	46.1	0.567	54.0	25.9	22.6
K^+	806	64	0.498	15.0	20.7	75.6	2.90	44.2	0.562	55.8	24.5	21.5
Na^+	856	66	0.303	10.3	13.1	76.0	2.35	25.6	0.568	59.4	16.9	13.8
Li^+	765	66	0.321	8.43	12.7	74.6	1.04	29.4	0.558	59.5	14.1	13.0
Ca^{2+}	759	63	0.343	8.59	12.9	74.1	1.01	31.4	0.559	55.8	14.2	13.1
Sr^{2+}	748	66	0.401	7.76	11.9	74.5	1.35	36.8	0.562	59.5	12.9	12.1
Ce^{3+}	642	63	0.195	5.51	10.6	75.3	1.41	21.6	0.529	53.2	9.39	10.4
La^{3+}	707	64	0.294	5.54	9.37	74.2	2.82	28.3	0.555	56.5	9.23	9.18

Table X. Dielectric parameters observed for beds of QAE-Sephadex beads in different salt forms dispersed in water at 25.0°C and phase parameters calculated from Eq. (2).

Specimen No.	Observed Dielectric Parameter							Calculated Phase Parameter				
	ε_l	ε_h	$\frac{\kappa_l}{\text{mS cm}^{-1}}$	$\frac{\kappa_h}{\text{mS cm}^{-1}}$	$\frac{f_0}{\text{MHz}}$	ε_a	$\frac{\kappa_a}{\mu\text{S cm}^{-1}}$	$\frac{\kappa_a}{\mu\text{S cm}^{-1}}$	Φ	ε_i	$\frac{\kappa_i}{\text{mS cm}^{-1}}$	$\frac{f_0}{\text{MHz}}$
1 Cl^-(*)	691	67	0.296	11.0	20.0	77.6	3.91	31.9	0.531	58.4	19.1	19.5
2 Br^-	639	67	0.249	10.3	20.7	78.3	5.23	29.4	0.515	57.4	18.1	20.1
3 I^-	639	66	0.251	6.72	12.8	78.3	2.58	29.0	0.521	55.9	11.6	12.9
4 ClO_3^-	752	67	0.294	8.91	14.1	78.3	5.40	29.1	0.546	58.4	15.0	14.0
5 BrO_3^-	686	65	0.182	8.26	14.8	78.7	1.86	20.6	0.525	54.0	14.0	14.5
6 NO_3^-	619	66	0.487	9.32	18.9	77.9	11.9	49.0	0.518	55.0	16.1	18.4
7 OH^-(*)	612	68	1.60	22.6	50.2	78.6	2.68	185	0.531	59.4	39.0	44.9
8 SO_4^{2-}	671	68	0.250	8.73	16.2	77.9	1.86	27.9	0.526	59.8	15.3	16.1
9 PO_4^{3-}	662	66	0.168	5.86	10.9	78.2	1.16	19.0	0.523	56.0	10.1	10.8

(*) The data refer to Table VII.

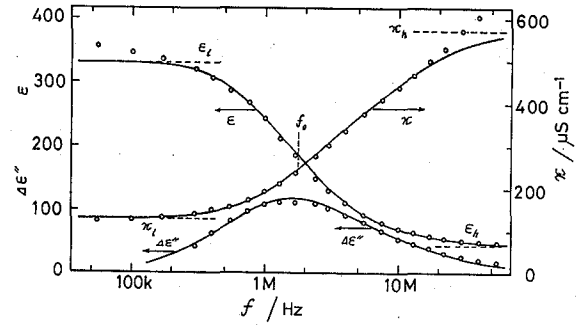

Fig. 7. Frequency dependence of relative permittivity ε, electrical conductivity κ, and loss factor $\Delta\varepsilon''$ for beds of Uniselec UR-30 beads in a hydrogen form dispersed in water at 24.8°C. Theoretical curves are calculated from Eq. (2).

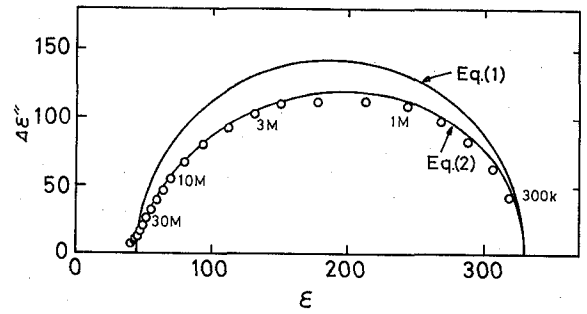

Fig. 8. Complex plane plots of complex relative permittivity and complex conductivity for beds of Uniselec UR-30 beads in a hydrogen form dispersed in water at 24.8°C. Theoretical curves are calculated from Eqs. (1) and (2). Numbers beside observed points are measuring frequencies.

Table XI. Dielectric parameters observed for a bed of Uniselec UR-30 beads in a hydrogen form at 24.8°C and phase parameters calculated form Eq. (2).

Observed Values		Values calculated from Eq. (2)	
ε_a	77.1		
κ_a/μS cm^{-1}	3.60	κ_a/μS cm^{-1}	20.7
dielectric parameters		Φ	0.538
ε_l	330.0	ε_i	24.8
ε_h	45.0	κ_i/μS cm^{-1}	781
κ_l/μS cm^{-1}	131		
κ_h/μS cm^{-1}	571		
f_0/MHz	1.56	f_0/MHz	1.75

Table XII. Dielectric parameters for Sephadex G-25 beads in KCl aqueous solutions at 23.4°C and the phase parameters calculated by using Eqs. (4) and (6). The volume fraction $\Phi=0.569$ in Table VIII is used in the calculations.

$\frac{[KCl]}{mequiv\ dm^{-3}}$	Observed Dielectric Parameter				Calculated Phase Parameters	
	ε_l	$\frac{\kappa_l}{\mu S\ cm^{-1}}$	ε_a	$\frac{\kappa_a}{\mu S\ cm^{-1}}$	ε_i	$\frac{\kappa_i}{\mu S\ cm^{-1}}$
0.16	74.5	31.67	80.9	26.82	67.4	35.7
0.80	76.0	75.04	80.9	116.3	68.9	50.6
1.60	75.8	127.3	79.9	234.3	66.0	69.3
2.00	75.5	159.2	79.6	291.0	65.8	87.4
3.00	77.2	231.4	82.5	426.3	66.7	126
4.00	78.2	297.4	82.9	551.4	66.4	160
8.00	—	618.1	—	1124	—	342

5.2.4 Ion-exchange beds in KCl solutions

Dielectric measurements were carried out on Sephadex G-25 beds dispersed in KCl solutions with different concentrations. At frequencies lower than 100 kHz, the permittivities ε showed remarkable increase with decreasing frequency owing to electrode polarization. At frequencies higher than 100 kHz, the permittivities ε and the conductivities κ showed values independent of frequency, being interpreted as the limiting values ε_l and κ_l for the dielectric relaxation in question of the ion-exchange beds. The observed dielectric data were analyzed by the procedure of Case B in Section 3 to obtain the phase parameters ε_i and κ_i. The results are summarized in Table XII. The analysis is made on the asumption that the volume fractions Φ in KCl solutions are equal to that for the specimen of the beads in a potassium form dispersed in water shown in Table VIII. The values of κ_i increase with the KCl concentrations in the outer continuous phase, while the values of ε_i remained unchanged and were equal to those in Table IV-(i), V-(i), VI and VIII.

Figure 9 shows the relation between κ_i and κ_a. In a range of low conductivity of the suspending medium, κ_i stands at a finite value which is independent of κ_a, while κ_i is linearly related to κ_a for higher values of κ_a.

For a system of a fixed negative charge phase in Donnan equilibrium with the ambient electrolyte solution phase, the conductivity κ_i can be expressed by the following approximate formulas for the limiting cases:[18,23]

$$\text{i)}\quad \kappa_i=\lambda_{bead}X, \qquad \text{for } C_a \ll X, \tag{8}$$

$$\text{ii)}\quad \kappa_i=(\lambda_{bead}{}^{+}+\lambda_{bead}{}^{-})C_a=\frac{\lambda_{bead}{}^{+}+\lambda_{bead}{}^{-}}{\lambda_a{}^{+}+\lambda_a{}^{-}}\kappa_a, \qquad \text{for } C_a \gg X, \tag{9}$$

where X, C and λ are the fixed charge density, the salt concentration, and the equivalent ionic conductance; and the subscripts $+$, $-$, a and i refer to the cations, the anions, the suspending medium, and the disperse phase, respectively. The observations shown in Fig. 9 can be reasonably interpreted in terms of Eqs. (8) and (9). Provided that $\lambda_{bead}{}^{Cl}$

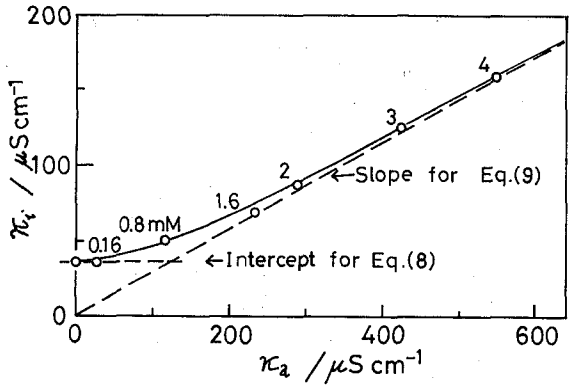

Fig. 9. Electrical conductivity κ_i of Sephadex G-25 beads against conductivity κ_a of the corresponding supernatants at 23.4°C. Numbers beside observed points are concentrations of KCl in mequiv dm^{-3}. Solid curve is derived from Donnan theory by use of values of X and λ_{bead} obtained.

is equal to λ_{bead}^{Na} as in an aqueous phase of KCl, we obtain the value of $\lambda_{bead}^{Cl}=\lambda_{bead}^{Na}=$ 20.7 S cm^2 equiv^{-1} from Eq. (9) by using the value of the slope $(\lambda_{bead}^{+}+\lambda_{bead}^{-})/(\lambda_a^{+}+\lambda_a^{-})$ in Fig. 9. The fixed charge density X is estimated to be 1.73 m equiv dm^{-3} from Eq. (8), which is too small value to be measured accurately by other methods such as titration.

5.2.5 Temperature dependence

Table XIII summarizes the dielectric parameters of high-frequency relaxations observed and the phase parameters deduced through the analysis of procedure of Case A in Section 3 for aqueous beds of high charge density type SP-Sephadex beads in a sodium form at three different temperatures.[20] The values of κ_i increase with increasing temperature T, whereas the values of ε_i and Φ are unchanged in spite of the increase in T. Although the permittivity ε_a of the supernatant decreases with increasing T, it seems that the poor accuracy of ε_i prevents us from finding out temperature dependence of ε_i.

5.2.6 Fixed charge density dependence

Figure 10 shows the frequency dependence of ε and κ for aqueous beds of sodium form sulfoethylated Sephadex G-25 with different fixed charge densities. In Table XIV are shown the dielectric parameters of the high-frequency relaxations and the phase parameters calculated by the procedure of Case A in Section 3.

The values of ε_i are somewhat lower than ε_a of the respective supernatants. In view of the accuracy of the analysis, the values of Φ and ε_i are seen to be almost unchanged irrespective of the fixed charge density X of the beads. This fact indicates that the degree of swelling and the degree of packing of the beads are scarcely influenced by the fixed charge density. This is supported experimentally by microscope observations of the unchanged radii of the beads after being subjected to sulfoethylation (Table III).

On the other hand, the conductivities κ_i are dependent upon X. The values of κ_i are plotted against X in Fig. 11. The figure shows that the value of κ_i increases linearly with X. This relation between κ_i and X is reasonable in the light of Eq. (8).

Table XIII. Dielectric parameters observed for beds of SP-Sephadex beads dispersed in water at 15.0, 25.0 and 35.0°C and phase parameters calculated from Eq. (2).

Temp. °C	Observed Dielectric Parameter							Calculated Phase Parameter				
	ε_l	ε_h	κ_l / mS cm^{-1}	κ_h / mS cm^{-1}	f_0 / MHz	ε_a	κ_a / μS cm^{-1}	κ_a / μS cm^{-1}	Φ	ε_i	κ_i / mS cm^{-1}	f_0 / MHz
15	842	67	0.213	8.17	11.6	81.8	1.48	19.9	0.553	56.3	13.3	11.2
25	738	65	0.450	10.1	16.4	79.0	3.26	44.8	0.548	54.7	16.6	15.9
35	730	65	0.660	11.8	19.6	76.6	4.59	63.2	0.556	56.6	19.4	18.7

Table XIV. Dielectric parameters for beds of SE-Sephadex beads in a sodium form dispersed in water at 25.0°C and phase parameters ealculated from Eq. (2). Specimen numbers are the same as those in Table III.

Specimen No.	Observed Dielectric Parameter							Calculated Phase Parameter				
	ε_l	ε_h	κ_l / mS cm^{-1}	κ_h / mS cm^{-1}	f_0 / MHz	ε_a	κ_a / μS cm^{-1}	κ_a / μS cm^{-1}	Φ	ε_i	κ_i / mS cm^{-1}	f_0 / MHz
1	515	70	0.0938	0.462	0.954	78.3	2.39	10.5	0.572	64.2	0.757	1.01
2	769	69	0.122	2.17	3.15	78.3	2.23	11.4	0.561	62.2	3.63	3.31
3	635	70	0.263	3.34	6.13	78.2	2.37	28.7	0.541	63.5	5.78	6.37
4	709	71	0.231	3.71	6.20	78.3	2.65	23.2	0.550	65.4	6.37	6.28
5	736	68	0.268	5.96	9.59	78.3	3.24	26.5	0.548	60.2	10.1	9.60
6	646	70	0.155	2.17	3.89	78.3	2.30	16.9	0.540	63.4	3.75	4.07

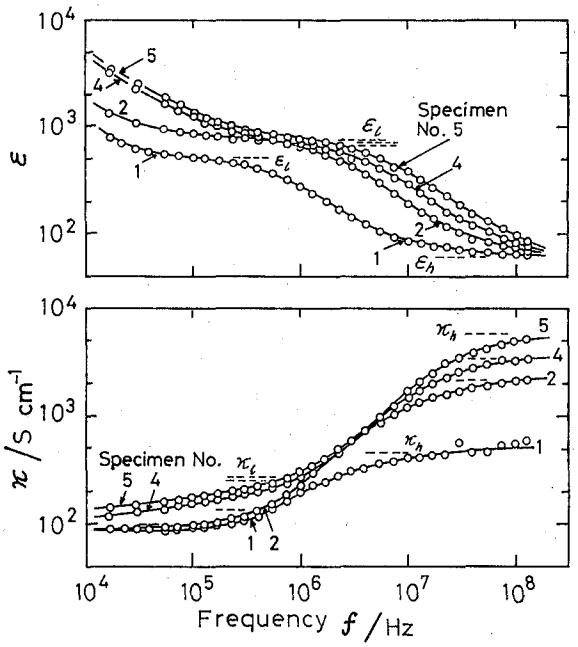

Fig. 10. Frequency dependence of relative permittivity ε and electrical conductivity κ for SE-Sephadex beads in a sodium form dispersed in water at 25.0°C. Specimen numbers beside the curves refer to those shown in Table XIV.

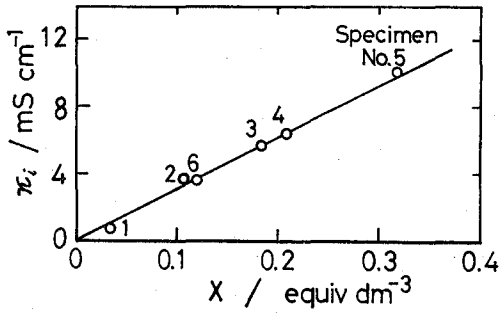

Fig. 11. Electrical conductivity κ_i of SE-Sephadex beads against fixed charge density $X=C_{bed}/\Phi$ of the beads at 25.0°C. Specimen numbers beside observed points refer to those shown in Table XIV.

5.3 Permittivity of ion-exchange beads

The permittivity ε_i of the dextran gel ion-exchange beads in Section 5.2 are less than ε_a of the supernatants. This finding is reasonable in view of the fact that the ion-exchange bead is a binary mixture: one component is a framework of dextran resins, the other being water molecules which permeate the gel beads. The permittivity of the beads for Sephadex G-25 is 67 on an average. According to Onsager's theory,[15,37] the relation of the permittivity ε_m of a binary mixture is given by

$$\frac{(\varepsilon_m-\varepsilon_A)(2\varepsilon_A\varepsilon_m+n_A{}^4)}{\varepsilon_A(2\varepsilon_m+n_A{}^2)^2}v+\frac{(\varepsilon_m-\varepsilon_B)(2\varepsilon_B\varepsilon_m+n_B{}^4)}{\varepsilon_B(2\varepsilon_m+n_B{}^2)^2}(1-v)=0, \qquad (10)$$

where the subscripts A and B refer to the components A and B, and v and n are the volume fraction of the component A and the refractive index, respectively. Numerical calculations of Eq. (10) showed that the curve of ε_m against v is approximated satisfactorily by a straight line[15] so far as values between 1 and 3 are assumed for n_A and n_B.

In view of such a character of Eq. (10), the permittivity of dextran gel matrix in water can readily be estimated as follows. Let the components A and B be the gel matrix and the water molecules, respectively. The value of ε_B is assumed to be 80, and the volume fraction v of the gel matrix to the resin beads to be 0.44, which was determined from the values $p=0.25$ measured by using D-glucose and $\Phi=0.57$ as an average value of Tables IV-(i) and VIII for Sephadex G-25. The value of ε_m in Eq. (10) is assumed to be 67 listed in Tables IV-(i), V-(i), VIII and XII. The permittivity ε_A of gel matrix in water was consequently estimated to be 58 in a state swollen with water.

To estimate the permittivity of gel matrix in an unswollen state, dielectric measurements were carried out for Sephadex G-25 beds in various organic solvents with different permittivities. The permittivities of these beds were obtained as frequency-independent values. Figure 12 shows plots of the permittivities of dextran gel beds in organic solvents against those of the respective supernatants. Circles in Fig. 12 show the observed values, which are represented roughly by a dashed line. The packing fraction of the beads can reasonably be assumed to be unchanged in different organic solvents, since a dextran gel is incapable of swelling in organic solvents.[36] Hence, an intersection of the dashed line and a solid line with a unity slope shows an iso-permittivity point, at which the permittivity is equal to that of the suspending medium. Thus, the permittivity of the gel beads was experimentally estimated to be 7 in these organic solvents. By using this value and the volume fraction $\Phi=0.57$, a theoretical curve is calculated from Eq. (2) and is shown with a dotted line in Fig. 12. The theoretical curve is in good agreement with the experimental values.

The permittivity of the Sephadex G-25 beads in aqueous phases is apparently large in comparison with the permittivity 7 which was determined in Fig. 12 for organic solvents.

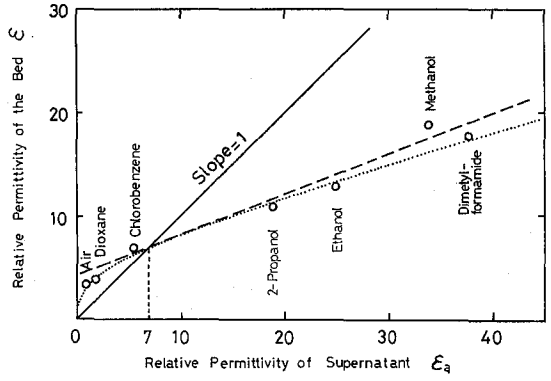

Fig. 12. Isopermittivity point method for Sephadex G-25 dispersed in organic solvents at 24.0°C. An intersection of the dashed line and a line with a unity slope shows the point at which permittivity of gel matrix of Sephadex G-25 is equal to that of suspending medium. The dotted curve is calculated from Eq. (2).

This finding is attributable to hydration of the gel matrix as is well known for hydrated biological materials, whose permittivities often show 10^1–10^2 in dielectric units.[38-41] Koide and Carstensen[42] measured the permittivity of the same material as that of the present study. They showed that the permittivity of dextran gel matrix with bound water was 37 dielectric units around 100 MHz. The result described here is consistent with that of these preceding studies.

5.4. Interaction of counter ions with fixed charges

5.4.1 Ion-exchangers with different dissociation groups

It is known from conductivity studies on suspensions of ion-exchanger[43,44] that the conductivities of resins are varied from species to species of the counter ions. The similar characteristics are also found in Tables VIII to X. Since no electrolyte is added to the specimens of Tables VIII to X, the values of κ_i are given by Eq. (8) as described in Section 5.2.4. The equivalent ionic conductances λ_{bead} of the counter ions in the beads were calculated from Eq. (8) by use of the values of κ_i and fixed charge density X, where $X=C_{bed}/\Phi$. The results are summarized in Table XV together with the equivalent ionic conductances λ_a in aqueous solutions.

It is obvious that the values of λ_{bead} obtained are smalle than the respective values of λ_a. In Table XV is also shown the relative decrement $f^*=1-\lambda_{bead}/\lambda_a$ of equivalent ionic conductance,[45,46] which represents the degree of increase in binding of the counter ions.

In the case of the cation exchangers of weakly charged Sephadex G-25 and highly charged SP-Sephadex C-25 (Table XV-(i) and (ii)), the values of f^* for hydrogen ions are relatively large in comparison with f^* of other univalent ions. In the case of Sephadex G-25, the values of f^* for alkyl ammonium ions decrease with increase in the chain length of the alkyl groups. The values of f^* for metallic ions depend on the valences of the counter ions. The relative magnitude of f^* of the metallic ions for Sephadex G-25 and SP-Sephadex is compared in the plot of λ_{bead} against λ_a (Fig. 13). All the observed points in Fig. 13 are located below a straight line with a unity slope. This fact indicates

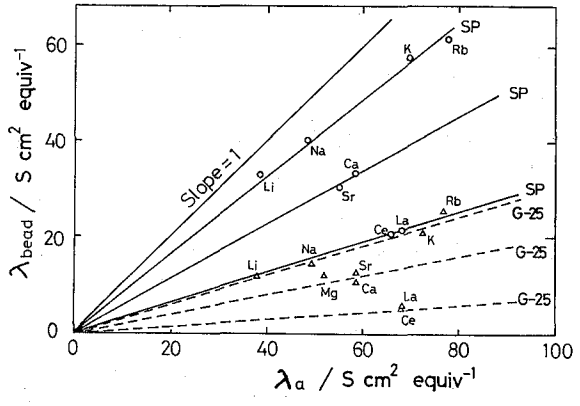

Fig. 13. Equivalent ionic conductance λ_{bead} of the ion-exchange beads against limiting equivalent ionic conductance λ_a in aqueous solutions. ○: Sephadex G-25 at 24.5°C, △: SP-Sephadex C-25 at 24.0°C.

Table XV. Equivalent ionic conductance λ_{bead} in the ion-exchange resins and λ_a in aqueous solutions.

(i) Sephadex G-25 at 24.5°C.

Salt form	λ_a / S cm² equiv⁻¹	λ_{bead} / S cm² equiv⁻¹	$f^*=1-(\lambda_{bead}/\lambda_a)$
H^+	347	39.9	0.89
Rb^+	76.8	25.2	0.67
K^+	72.6	20.7	0.71
Na^+	49.5	14.7	0.70
Li^+	38.2	11.7	0.69
NH_4^+	72.6	23.5	0.68
Me_4N^+	44.4	13.6	0.69
n-Bu_4N^+	19.2	6.85	0.64
n-Am_4N^+	17.2	7.20	0.58
Mg^{2+}	52.3	12.3	0.76
Ca^{2+}	58.7	10.7	0.82
Sr^{2+}	58.7	12.7	0.78
Ce^{3+}	68.8	5.18	0.92
La^{3+}	68.8	5.81	0.91

(ii) SP-Sephadex at 24.0°C.

Salt form	λ_a / S cm² equiv⁻¹	λ_{bead} / S cm² equiv⁻¹	$f^*=1-(\lambda_{bead}/\lambda_a)$
H^+	345	217	0.37
Rb^+	77.8	61.7	0.21
K^+	69.8	57.8	0.17
Na^+	48.7	40.3	0.17
Li^+	38.9	33.1	0.15
Ca^{2+}	58.5	33.4	0.43
Sr^{2+}	55.2	30.5	0.45
Ce^{3+}	65.1	20.9	0.68
La^{3+}	68.2	21.5	0.68

(iii) CM-Sephadex at 25.0°C.

Salt form	λ_a / S cm² equiv⁻¹	λ_{bead} / S cm² equiv⁻¹	$f^*=1-(\lambda_{bead}/\lambda_a)$
Cl^-	76.35	30.5	0.60
Br^-	78.14	28.0	0.64
I^-	78.64	18.1	0.77
ClO_4^-	64	24.6	0.62
BrO_4^-	56	22.1	0.61
NO_3^-	71.46	25.0	0.65
OH^-	198.3	62.2	0.69
SO_4^{2-}	80.02	24.2	0.70
PO_4^{3-}	—	15.9	—

Table XVI. Comparison of equivalent ionic conductance λ_{bead} in SP-Sephadex beads which are regarded as homogeneous spheres to λ_{Na} in aqueous solutions.

Temp. °C	λ_a S cm² equiv⁻¹	λ_{bead} S cm² equiv⁻¹	$f^*=1-(\lambda_{bead}/\lambda_a)$
15	41.4	31.4	0.24
25	50.1	38.9	0.22
35	63	46.1	0.27

decrease of activity of the counter ions. The dependence of f^* on valence of the counter ions is represented by linear relation of the respective ions of the same valence. Since the solid lines for SP-Sephadex are located above the dotted lines for Sephadex G-25, it is seen that the interaction between the fixed charges and the counter ions is stronger for Sephadex G-25 than for SP-Sephadex. This feature is considered to be due to difference of dissociation nature between sulfoxyl groups and carboxyl groups.

In the case of highly charged anion exchanger QAE-Sephadex (Table XV-(iii)), the value of f^* of hydroxyl ions is large in comparison with f^* of other univalent counter ions. This fact is compared to the character of f^*-value of hydrogen ions in the case of the cation exchange resins, suggesting an interaction due to hydrogen bonding. Most of the values of f^* lie between 0.6 and 0.65, which can be regarded as unchanged in view of the accuracies of f^*-values.

These observations on f^* in Table XV are consistent with ion-binding phenomena observed for polyelectrolyte solutions.[45-48]

5.4.2 Temperature dependence

From the value of κ_i for SP-Sephadex beds in Table XIII, the values of λ_{bead} were calculated from Eq. (8) by giving the values of X. The results are shown in Table XVI together with the values of $f^*=1-(\lambda_{bead}/\lambda_a)$ and λ_{Na} of sodium ions in the continuous medium. Though the values of λ_{bead} are seen to increase with T, the values of f^* show

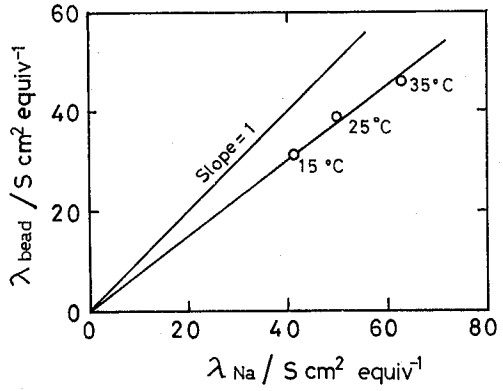

Fig. 14. Equivalent ionic conductance λ_{bead} of the ion-exchange beads against limiting equivalent ionic conductance λ_{Na} of in aqueous solutions at different temperatures.

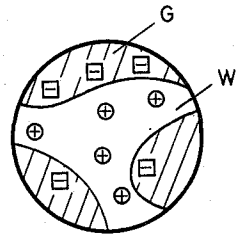

Fig. 15. Sponge-like model of a dextran gel ion-exchange bead. G: dextran gel matrix, W: interstitial water, ⊕: counter ions, ⊟: fixed charges.

an inappreciable change with T. That is, the plot of λ_{bead} against λ_a is linear as shown in Fig. 14. This fact suggests that the interaction between fixed sulfoxyl groups and the counter sodium ions is almost unchanged in the temperature range in Table XIII.

5.4.3 Dependence on fixed charge density

As shown in Fig. 11, the value of κ_i increases linearly with X. The linear relation is reasonably understood from Eq. (8) with a value of $\lambda_{bead}=30.9$ S cm^2 equiv^{-1}. The unchanged values of λ_{bead} indicate almost no dependence of the interaction of the fixed sulfoxyl groups with sodium ions on the fixed charge density.

As is often discussed, ion-exchange beads consist of gel matrix and the interstitial water, being compared to a sponge immersed in water.[48] This model can be drawn schematically in Fig. 15. According to the model, the ion migration takes place only in the interstices of the gel matrix. The equivalent ionic conductance λ_{int} in the interstices can be written as

$$\lambda_{int}=\lambda_{bead}/(1-v), \tag{11}$$

where $v=p/\Phi$ is the volume fraction of the gel matrix in the ion-exchange beads.

By using the values of κ_i and Φ in Table XIV, and C_{bed} and p in Table III, the values of λ_{bead} and λ_{int} for sodium ions are calculated from $X=C_{bed}/\Phi$, Eq. (8), $v=p/\Phi$ and Eq. (11). The results are summarized in Table XVII. Using the limiting equivalent ionic conductance of sodium ions $\lambda_{Na}=50.1$ S cm^2 equiv^{-1} in the continuous medium at 25°C, the values of f^* are shown to be decreased to 0.85. Since the decrease in equivalent conductance in aqueous phases to this degree is usually observed in electrolyte

Table XVII. Equivalent ionic conductance λ_{bead} in SE-Sephadex beads which are regarded as homogeneous spheres and λ_{int} in the interstics of gel matrix of SE-Sephadex beads at 25.0°C.

Specimen	λ_{bead} / S cm^2 equiv^{-1}	λ_{int} / S cm^2 equiv^{-1}	$f^*_{int}=1-(\lambda_{int}/\lambda_a)$
1	22	34	0.32
2	33.9	47.7	0.05
3	31.4	43.4	0.13
4	30.5	42.2	0.16
5	31.8	42.4	0.15
6	30.5	42.4	0.15

solutions,[49] it is infered that there exists no specific affinity between the counter sodium ions and the fixed sulfoxyl groups. This feature concerning the sulfoxyly groups is reasonably understood in conformity with their nature of strong electrolytes.

5.4.4 Comparison of interaction of counter ions between carboxyl and sulfoxyl type ion-exchangers

The linear relation between λ_{bead} and λ_a obtained for both the SP-Sephadex and Sephadex G-25 in Fig. 13 is at first sight strange since carboxyl type ion-exchangers are often said to make chelate formation with multivalent ions[48] and so are expected to have a specific interaction with counter ions of multivalence. The conceivable reason for these unexpected results is that the fixed charge density is too low for chelate formation. To check the validity of this explanation, dielectric measurements were carried out for CM-Sephadex, carboxyl type ion-exchange beads with higher fixed charge density. Table XVIII summarizes the dielectric parameters observed for CM-Sephadex and SP-Sephadex beds in different salt forms dispersed in water and the respective phase parameters calculated from Eq. (2). The values of λ_{int} were estimated from Eqs. (8) and (11) and summarized in Table XIX together with the respective values of $f^*_{int}=1-(\lambda_{int}/\lambda_a)$.

In the case of the SP-Sephadex, it is seen that the activity of the counter ions shows no decrease for univalent sodium ion and a slight decrease for the bivalent ions. On the other hand, in the case of the CM-Sephadex, the value of f^*_{int} of the counter sodium ion is a little larger than f^*_{int} of the bivalent ions of the SP-Sephadex. The values of f^*_{int} of the counter bivalent ions of the CM-Sephadex are close to unity. It is plausible that selective bindings comparable to an ion pair or a chemical bonding are formed between the bivalent ions and the fixed charges for the C-MSephadex. This binding character of the fixed charge is extremely strong with cupric ions. These findings may be attributed to chelate binding nature of carboxyl type ion-exchangers.

6. CONCLUSION

Several equations were derived in a form convenient for practical application to dielectric data on the basis of two theoretical equations (1) and (2) of interfacial polarization. The several relations derived were applied to the observed data of dense sediments of ion-exchange beads in aqueous solutions to evaluate the relative permittivity and the electrical conductivity of the disperse phases. Comparison between Eqs. (1) and (2) showed that Eq. (2) for concentrated disperse systems represented satisfactorily the frequency dependence of the observed data. For aqueous suspensions in different concentrations of ion-exchange beads, the values of ε_i and κ_i obtained by the analysis were unchanged irrespective of the concentrations. This consistent result indicates the validity of the method of analysis.

In terms of the values of ε_i and κ_i evaluated by the method of analysis, dielectric properties were compared among several ion-exchange beads of dextran gel matrix carrying different dissociation groups. Preconditionings with electrolyte solutions were performed on the ion-exchange beads to be measured. It was found that the preconditionings caused the conversion of salt forms and that the value of κ_i were characteristic of the salt forms. On the other hand, the values of Φ and ε_i showed somewhat varied values for different ion-exchangers, being almost independent of the salt forms.

Table XVIII. Dielectric parameters observed for beds of SP-Sephadex and CM-Sephadex beads in different salt forms dispersed in water at 25.0°C and phase parametes calculated from Eq. (2).

Salt form	Observed Dielectric Parameter							Calculated phase Parameter				
	ε_l	ε_h	$\frac{\kappa_l}{\mathrm{mS\ cm^{-1}}}$	$\frac{\kappa_h}{\mathrm{mS\ cm^{-1}}}$	$\frac{f_0}{\mathrm{MHz}}$	ε_a	$\frac{\kappa_a}{\mu\mathrm{S\ cm^{-1}}}$	$\frac{\kappa_a}{\mu\mathrm{S\ cm^{-1}}}$	Φ	ε_i	$\frac{\kappa_i}{\mathrm{mS\ cm^{-1}}}$	$\frac{f_0}{\mathrm{MHz}}$
	SP-Sephadex C-25											
Na^+	804	68	0.386	9.59	14.1	77.8	3.11	35.1	0.561	60.9	15.9	13.9
Ca^{2+}	714	65	0.371	7.29	12.1	78.3	1.25	37.5	0.547	55.1	12.0	11.9
Zn^{2+}	787	69	0.324	6.88	10.1	78.0	1.89	29.7	0.560	62.4	11.5	10.3
Cu^{2+}	650	64	0.210	6.71	12.8	78.3	2.52	24.1	0.521	52.4	11.4	12.5
	CM-Sephadex C-25											
Na^+	752	68	0.418	12.6	19.9	78.0	5.86	41.2	0.546	60.4	21.5	20.1
Ca^{+2}	461	67	0.170	1.55	4.34	78.7	4.20	25.0	0.500	56.5	2.77	4.27
Zn^{2+}	581	68	0.117	0.988	1.91	78.1	3.70	13.1	0.547	60.3	1.66	2.00
Cu^{2+}	192	61	0.0116	0.0310	0.197	78.2	1.24	3.10	0.466	44.8	0.0529	0.207

Table XIX. Equivalent ionic conductance λ_{int} in the interstices of gel matrix of SP-Sephadex and CM-Sephadex beads and λ_a in aqueous solutions at 25.0°C.

Specimen	λ_{int} / S cm² equiv⁻¹	λ_a / S cm² equiv⁻¹	$f^*_{int}=1-(\lambda_{int}/\lambda_a)$
	SP-Sephadex C-25		
Na^+	50.5	50.1	0.0
Ca^{2+}	42.5	59.5	0.29
Zn^{2+}	40.7	52.8	0.23
Cu^{2+}	42.2	53.6	0.22
	CM-Sephadex C-25		
Na^+	29.9	50.1	0.40
Ca^{2+}	5.47	59.5	0.908
Zn^{2+}	4.07	52.8	0.924
Cu^{2+}	0.974	53.6	0.98

A similar analysis was also carried out on a series of specimens with different concentrations of KCl in the continuous medium. The values of κ_i increased with the KCl concentration as expected from the theory of Donnan equilibrium. From the analysis on the basis of the Donnan theory, the fixed charge density was estimated to be 1.73 equiv dm^{-3}, which is too small to be determined accurately by other method. The values of ε_i for this series of specimens were unchanged and equal to those without addition of KCl.

From the values of ε_i obtained, the permittivity of the gel matrix was estimated to be more than 50 dielectric units in a state swollen with water, while it was less than 10 dielectric units in an unswollen state. This discrepancy of the permittivity is considered to be due to hydration effect of the dissociation groups.

The equivalent ionic conductance λ_{bead} of different counter ions were estimated from the values of κ_i. From the plots of λ_{bead} against λ_a in the continuous medium, it is obvious that an interaction between the fixed charges and the counter ions are dependent on valence of the counter ions and that the interaction is stronger for carboxyl groups than for sulfoxyl groups. In the case of CM-Sephadex carrying carboxyl groups in concentration of 10^{-1} equiv dm^{-3}, it is seen that the interaction with bivalent ions is sufficiently strong to form specific binding close to ion pair or chemical bonding between the fixed charge and the ions.

APPENDIX

The theoretical formulas appearing in Ref. 1 relevant to the data analysis in the text are summarized as follows.

A.1. Equation for dilute systems

Numerical values of κ_a can be obtained from the following equation by computer-searching, provided that the values of ε_l, ε_h, κ_l, κ_h and ε_a are given from the observed data.

$$H(\kappa_a)\equiv\sqrt{\frac{\kappa_l\varepsilon_a-\kappa_a\varepsilon_l}{\kappa_h\varepsilon_a-\kappa_a\varepsilon_h}}-\frac{\kappa_a}{\varepsilon_a}\cdot\frac{\varepsilon_l-\varepsilon_h}{\kappa_h-\kappa_l}=0. \tag{A.1}$$

By using the value of κ_a obtained, the values of Φ, ε_i and κ_i are calculated from the following equations (A.2)–(A.4) in sequence.

$$\Phi=\frac{\varepsilon_a\varepsilon_h(\kappa_l-\kappa_a)^2+(\varepsilon_a-\varepsilon_h)(\varepsilon_a\kappa_l^2-\varepsilon_l\kappa_a^2)}{(\varepsilon_a\kappa_l-\varepsilon_h\kappa_a)^2+(\varepsilon_l-\varepsilon_h)(2\varepsilon_a+\varepsilon_h)\kappa_a^2}, \tag{A.2}$$

$$\varepsilon_i=\varepsilon_a\frac{\Phi(2\varepsilon_a+\varepsilon_h)-2(\varepsilon_a-\varepsilon_h)}{\Phi(2\varepsilon_a+\varepsilon_h)+(\varepsilon_a-\varepsilon_h)}, \tag{A.3}$$

$$\kappa_i=\kappa_a\frac{\Phi(2\kappa_a+\kappa_l)-2(\kappa_a-\kappa_l)}{\Phi(2\kappa_a+\kappa_l)+(\kappa_a-\kappa_l)}. \tag{A.4}$$

The relaxation frequency f_0 is given by

$$f_0=\frac{(2+\Phi)\kappa_a+(1-\Phi)\kappa_i}{(2+\Phi)\varepsilon_a+(1-\Phi)\varepsilon_i}\cdot\frac{1}{2\pi\epsilon_v}. \tag{A.5}$$

A.2. Equation for concentrated systems

Provided that ε_l, ε_h, κ_l, κ_h and ε_a are given from the observed data, we can obtain the value of κ_a by means of computer-searching for the following equation:

$$\begin{aligned}J(\kappa_a)\equiv&\left[3-\left(2+\frac{\varepsilon_a}{\varepsilon_h}\right)C\right](1-DC)\kappa_h\\&-3\{\kappa_l-[\kappa_a(D-1)+\kappa_l]C\}(1-C)\\&+\kappa_a\left(1-\frac{\varepsilon_h}{\varepsilon_a}\right)C(1-DC)=0,\end{aligned} \tag{A.6}$$

where

$$C=\frac{-Q-\sqrt{Q^2-4PR}}{2P} \tag{A.7}$$

$$P=\left(\frac{\kappa_a}{\kappa_l}+2\right)\varepsilon_lD-3[\varepsilon_hD-\varepsilon_a(D-1)]D+\left(\frac{\kappa_l}{\kappa_a}-1\right)\varepsilon_aD, \tag{A.8}$$

$$Q=3[2\varepsilon_hD-\varepsilon_a(D-1)]-\left[\left(\frac{\kappa_a}{\kappa_l}+2\right)D+3\right]\varepsilon_l-\left(\frac{\kappa_l}{\kappa_a}-1\right)\varepsilon_aD, \tag{A.9}$$

$$R=3(\varepsilon_l-\varepsilon_h), \tag{A.10}$$

$$D=\left(\frac{\varepsilon_a\kappa_l}{\varepsilon_h\kappa_a}\right)^{1/3}. \tag{A.11}$$

Using the values of κ_a thus calculated, the values Φ, ε_i and κ_i are obtained from the following equations (A.12)–(A.14) in sequence.

$$\Phi=1-\left(\frac{\varepsilon_a}{\varepsilon_h}\right)^{1/3}C, \tag{A.12}$$

$$\varepsilon_i=\frac{\varepsilon_h-\varepsilon_aC}{1-C} \tag{A.13}$$

and

$$\kappa_i=\frac{\kappa_l-\kappa_aDC}{1-DC} \tag{A.14}$$

A theoretical expression for the relaxation frequency has not been derived yet in an analytical form. By computer-searching, we can obtain the numerical values of f_0.

ACKNOWLEDGMENT

The authors wish to thank to Dr. K. Asami and Dr. S. Sasaki for helpful suggestions.

REFFRENCES

(1) T. Hanai, A. Ishikawa, and N. Koizumi, *Bull. Inst. Chem. Res., Kyoto Univ.*, **55**, 376 (1977).
(2) A. Ishikawa, T. Hanai, and N. Koizumi, *Jpn. J. Appl. Phys.*, **20**, 79 (1981).
(3) T. Hanai, T. Imakita, and N. Koizumi, *Colloid and Polymer Sci.*, **260**, 1029 (1982).
(4) C. W. Einolf Jr., and E. L. Carstensen, *J. Phys. Chem.*, **75**, 1091 (1971).
(5) C. T. O'Konski, *J. Phys. Chem.*, **64**, 605 (1960).
(6) G. Schwarz, *J. Phys. Chem.*, **66**, 2636 (1962).
(7) J. M. Schurr, *J. Phys. Chem.*, **68**, 2407 (1964).
(8) J. C. Maxwell, "A Treatise on Electricity and Magnetism", 3rd ed, Clarendon Press, Oxford, 1891, Vol. I, Chap. IX Art., 310–314, pp. 435–441.
(9) V. I. Frolov, N. P. Kuznetsova, L. R. Gudkin, and R. N. Mishayeva, *Vysokomol. Soedin.*, **A19**, 984 (1977).
(10) S. B. Sachs, and K. S. Spiegler, *J. Phys. Chem.*, **68**, 1214 (1964).
(11) K. Arulanandan, S. S. Smith and K. S. Spiegler, in "Polyelectrolytes", E. Sélégny Ed., D. Reidel Publishing Company, Dordrecht-Holland, 1974, p. 301.
(12) M. C. Sauer, P. F. Southwick, K. S. Spiegler, and M. R. J. Wyllie, *Ind. Eng. Chem.*, **47**, 2187 (1955).
(13) K. S. Spiegler, R. L. Yoest, and M. R. J. Wyllie, *Discuss. Faraday Soc.*, **21**, 174 (1956).
(14) K. W. Wagner, *Arch. Electrotech.*, **2**, 371 (1914).
(15) T. Hanai, in "Emulsion Science", P. Sherman Ed., Academic Press, London and New York, 1968, Chap. 5, p. 353.
(16) T. Hanai, *Kolloid Z.*, **171**, 23 (1960).
(17) T. Hanai, *Kolloid Z.*, **175**, 61 (1961).
(18) A. Ishikawa, T. Hanai, and N. Koizumi, *Jpn. J. Appl. Phys.*, **21**, 1762 (1982).
(19) A. Ishikawa, T. Hanai, and N. Koizumi, *Jpn. J. Appl. Phys.*, **22**, 942 (1983).
(20) A. Ishikawa, T. Hanai, and N. Koizumi, Colloid and Polymer Sci., **263**, (1985) in press.
(21) J. Peška, J. Štamberg, and J. Hradil, *Angew. Makromol. Chem.*, **53**, 73 (1976).
(22) Technical literature provided from Phamacia Fine Chemicals.
(23) E. L. Carstensen, H. A. Cox, *Jr.*, W. B. Mercer, and L. A. Natale, *Biophys. J.*, **5**, 289 (1965).
(24) A. Ishikawa, T. Hanai, and N. Koizumi, *Colloid and Polymer Sci.*, **262**, 477 (1984).
(25) H. P. Schwan, in "Determination of Biological Impedance", Physical Techniques in Biological Research, Vol. VI, Part B, W. L. Nastuk Ed., Academic Press, New York and London, 1963, p. 434.
(26) K. Asami, A. Irimajiri, T. Hanai, and N. Koizumi, *Bull. Inst. Chem. Res. Kyoto Univ.*, **51**, 231 (1973).
(27) H. P. Schwan, G. Schwarz, J. Maczuk, and H. Pauly, *J. Phys. Chem.*, **66**, 2626 (1962).
(28) I. M. Williams and A. M. James, *J. Chem. Soc. Faraday Trans.*, **172**, 803, (1976).
(29) C. Ballario, A. Bonincontro, and C. Cametti, *J. Colloid and Interface Sci.*, **54**, 415 (1976).
(30) C. Ballario, A. Bonincontro, and C. Cametti, *J. Colloid and Interface Sci.*, **72**, 304 (1979).
(31) S. Sasaki, A. Ishikawa, and T. Hanai, *Report Prog. Polymer Phys. Jpn.*, **23**, 99 (1980).
(32) S. Sasaki, A. Ishikawa, and T. Hanai, *Biophys. Chem.*, **14**, 45 (1981).
(33) W. E. Vaughan, in "Dielectric Properties and Molecular Behaviour", N. Hill, W. E. Vaughan and A. H. Price Eds., Van Nostrand Reinhold Company, London, 1969, Chap. 2.
(34) E. H. Grant, R. J. Sheppard, and G. P. South, "Dielectric Behaviour of Biological Molecules in Solution", Clarendon Press, Oxford, 1978, p. 62.
(35) T. Hanai and N. Koizumi, *Bull. Inst. Chem. Res., Kyoto Univ.*, **54**, 248 (1976).
(36) L. Fischer, "An Introduction to Gel Chromatography", North-Holland Publishing Company, Amsterdam, 1969.

(37) L. Onsager, *J. Amer. Chem. Soc.*, **58**, 1486 (1936).
(38) R. Pethig, "Dielectric and Electronic Propejties of Biological Materials", John Wiley & Sons Ltd., Chichester, New York, Brisbane and Toronto, 1979, p. 175.
(39) D. Rosen, *Trans. Faraday Soc.*, **59**, 2178 (1963).
(40) S. Takashima and H. P. Schwan, *J. Phys. Chem.*, **69**, 4176 (1965).
(41) G. Brausse, A. Mayer, T. Nedetzka, P. Schlecht, and H. Vogel, *J. Phys. Chem.*, **72**, 3098 (1968).
(42) G. T. Koide and E. L. Carstensen, *J. Phys. Chem.*, **80**, 55 (1976).
(43) Von E. Jenckel and H. V. Lillin, *Kolloid Z.*, **146**, 159 (1956).
(44) R. Revy and A. Katchalsky, *J. Colloid and Interface Sci.*, **42**, 366 (1973).
(45) S. A. Rice and M. Nagasawa, "Polyelectrolyte Solutions", Academic Press, London and New York, 1961, p. 427.
(46) M. Nagasawa, in "Polyelectrolytes", E. Sélégny Ed., D. Reidel Publishing Company, Dordrecht-Holland, 1972, p. 57.
(47) F. Oosawa, "Polyelectrolytes", Mercel Dekker, Inc., New York, 1971, p. 71.
(48) F. Helfferich, "Ion Exchange", McGraw-Hill Book Company, New York, San Francisco, Toronto and London, 1962.
(49) "Landolt-Börnstein Zahrlenwerte und Funktionen aus Physik, Chemie, Astronomie, Geophysik, Technik", Band 7-II, Springer-Verlag 1960, p. 259.